BULLETIN OF THE POLISH ACADEMY OF SCIENCES
TECHNICAL SCIENCES, Vol. 71(3), 2023, Article number: e145564
DOI: 10.24425/bpasts.2023.145564

MATERIAL SCIENCE AND NANOTECHNOLOGY

Electrochemical behavior and morphology of selected sintered samples of $Mg_{65}Zn_{30}Ca_4Pr_1$ alloy

Bartłomiej HRAPKOWICZ [1], **Sabina LESZ** [1]*, **Aleksandra DRYGAŁA** [1], **Małgorzata KAROLUS** [2], **Klaudiusz GOŁOMBEK** [3], **Rafał BABILAS** [1], **Julia POPIS** [1], **Adrian GABRYŚ** [1], **Katarzyna MŁYNAREK-ŻAK** [1] and **Dariusz GARBIEC** [4]

[1] Department of Engineering Materials and Biomaterials, Silesian University of Technology, ul. Konarskiego 18A, 44-100 Gliwice, Poland
[2] Institute of Materials Engineering, University of Silesia, ul. Pułku Piechoty 75 1a, 41-500 Chorzów, Poland
[3] Materials Research Laboratory, Silesian University of Technology, ul. Konarskiego 18a, 44-100 Gliwice, Poland
[4] Łukasiewicz Research Network – Poznań Institute of Technology, ul. Ewarysta Estkowskiego 6, 61-755 Poznan, Poland

Abstract. In order to investigate the effect of the milling time on the corrosion resistance of the $Mg_{65}Zn_{30}Ca_4Pr_1$ alloy, powders of the alloy were prepared and milled for 13, 20, and 70 hours, respectively. The samples were sintered using spark plasma sintering (SPS) technology at 350°C and pressure of 50 MPa. The samples were subjected to potentiodynamic immersion tests in Ringer's solution at 37°C. The obtained values of E_{corr} were –1.36, –1.35, and –1.39 V, with polarization resistance R_p = 144, 189, and 101 Ω for samples milled for 13, 20 and 70 h, respectively. The samples morphology showed cracks and pits, thus signaling pitting corrosion.

Key words: magnesium; rare-earth elements; SPS; corrosion.

1. INTRODUCTION

Permanent implants are mainly used in orthopedics, but sometimes they need to be removed. Re-operation is difficult and carries the risk of complications in the form of infection and inflammation. Symptoms such as infection or metal irritation are indications for immediate removal [1, 2]. A solution seems to be the introduction of biodegradable materials capable of self-decomposition [3–5], which could be resorbed to supplement bone union and negate the need for reoperation [6].

Magnesium materials have long attracted the attention of scientists because of their specific characteristics. They are light and have mechanical properties like human bones [7–10]. Furthermore, magnesium materials are susceptible to modifications that can significantly change and select their properties [3,7,11]. Elements such as zinc and calcium have long been used to improve magnesium alloys, both in terms of mechanical and structural properties and, above all, corrosion resistance [12–15]. Rare earth elements drastically increase the mechanical properties of magnesium alloys [16–18], while many of them are toxic, which prevents their use for medical purposes. However, it is worth considering that some of them are characterized by low or negligible toxicity, which in a small amount can significantly improve the properties of the alloy [19, 20]. Recently conducted studies about the effect on selected REE accumulation reveal they may be stored in various organs in tissues. The amount of time needed for their metabolization differs depending on the area they are located in. For example, the effect of the elements such as gadolinium, praseodymium, neodymium to name but a few, has been studied in Sprague-Dawley rats. As reported by Cao [21], those elements accumulate mainly in blood, hair, spleen, liver, and bones. These accumulations of low concentrations are said to be reversible in blood and hair, although not in spleen, liver, and bones. However, literature from the second half of the 20th century mentions the retention of praseodymium in the liver or kidneys of mice and rats with biological half-lifetime of around 5–10 days. As for the bones, it is mentioned the accumulation is reversible, although it takes a considerable time assumed to be around 3600 days [22–24].

The production of materials with such different melting points presents some technical problems that are difficult to overcome in the production of alloys by traditional methods, such as casting. Using the phenomenon of solid-state diffusion, an alloy can be obtained with a given chemical composition without the need to melt it [25, 26]. The powders obtained in this way can be relatively easily consolidated by incremental methods or by sintering. Another advantage of such a solution is the possibility of obtaining elements in nearly finished shape, making finishing via machining or other techniques either negligible or obsolete [27–29].

Mechanical synthesis or mechanical alloying is a method which uses cyclical welding, fracturing, and re-welding of powder particles. Thanks to a high degree of possible customization, the properties of resulting alloys can be finely tuned in response to the role the material should employ. Many parameters of the process, such as milling time, milling medium or atmosphere, to mention but a few, have a critical effect on the

*e-mail: sabina.lesz@polsl.pl

Manuscript submitted 2022-09-14, revised 2023-02-17, initially accepted for publication 2023-02-27, published in June 2023.

obtained powdered alloy properties. As it was mentioned above, the MA method consists of a solid-state processing via dry high energy-ball milling (usually, wet method can be used as well). It is possible to obtain materials with amorphous, crystalline, or nano-crystalline structure. The resulting powders can be compacted to obtain appropriate products in a form close to a net-shape [30, 31]. One such method is spark plasma sintering (SPS), which is advantageous for such applications due to its ability to produce ultra-fine structure without pores or defects. Moreover, SPS allows for fast densification of the powder at lower temperatures as compared to traditional methods, thus facilitating higher control over the expected microstructure [28, 29].

With materials for medical applications, especially orthopedic or dental ones, it is very important to determine their behavior in corrosive conditions of the human body and even more so with a biodegradable material. Consequently, there is much work related to assessing the corrosion behavior of Mg and its alloys. Due to its corrosion resistance, Mg-based alloys are problematic, as it is one of the most reactive engineering materials. Its behavior results from a high intrinsic tendency for dissolution and the presence of impurities and/or secondary phases, causing local micro-galvanic corrosion. The former is inhibited by a weak film occurring in corrosive environments on the Mg surface. Hence, it is vital to address those issues via the production method and by alloying [10].

In this work, the Mg-Zn-Ca-Pr alloy was prepared by the powder metallurgy method with high-energy ball milling and was subjected to the spark-plasma sintering process. The samples prepared in this way were earlier studied in [24] and subsequently tested for their corrosion resistance. Potentiodynamic immersion tests were carried out to determine the corrosion current, corrosion potential, and using extrapolation of the Tafel anode and cathode slopes, polarization curves were determined from which corrosion resistance can be deduced.

2. MATERIALS AND METHODS

The research material was prepared by high-energy mechanical milling in a SPEX 8000D shaker ball mill. The powder mixture was prepared from pure Mg, Zn, Pr powders (99.99% wt.%) and pieces of Ca (99.99% wt.%).

The powders were milled successively for 13, 20, and 70 h using the 8000D Mixer/Mill–Dual High Energy Ball Mill. The stainless-steel vials with the powder were milled for varying cycles for 1 h and 30 min break to cool down the milled mixture. Ball-to-powder ratio was 10:1. All processes were performed under an argon protective atmosphere.

The obtained powders were sintered via Spark-Plasma Sintering HP D 25/3 device with 350°C sintering temperature and 50 MPa of compaction pressure, four minutes holding time, in a graphite die (Graphite, 2334-grade). The heating rate was 50°C·min^{-1} up to 300°C and 25°C·min^{-1} from 300°C to 350°C.

The obtained specimens of 20 mm diameter were then cut and prepared for immersion tests. Corrosion testing was carried out in Ringer solution at 37°C, simulating the natural environment of the human body, on Autolab 302N potentiostat equipped with a cell containing the reference electrode (saturated calomel electrode – SCE) and the counter electrode (platinum rod). The samples were tested by 3600 s of open-circuit potential E_{OCP} at a scan rate of 1 mV·s^{-1}. The polarization curves with Tafel's extrapolation were determined after stabilization time.

To assess the corrosion effects surface images were collected by means of a scanning electron microscope (SEM – Supra 35 Zeiss). Chemical composition was analyzed using energy-dispersive spectroscopy (EDS) and characterized via the Pathfinder 2.4 X-ray Microanalysis Software.

3. RESULTS AND DISCUSSION

3.1. Scanning electron microscopy – morphology and qualitative chemical composition analysis

In Fig. 1 the surface of the samples before and after the immersion tests can be seen. The samples after bending test [24] but before corrosion test feature various cracks (Fig. 1a–c) although the surface after corrosion is much more evolved in comparison (Fig. 1d–f). Fractures present for 13-, 20- and 70-hour samples have brittle characteristics; however, the visible differences between images in Fig. 1a and 1b and Fig. 1c may be caused by the debonding of particles during the sintering process [32]. It may be attributed to the size of the crystallites of $MgZn_2$ phases, which is considerably greater after 70 hours when compared to the samples after 13 and 20 hours [27]. The morphology of the samples after corrosion is well-developed, with many pits, creases, and cracks, suggesting pitting corrosion. The brighter patches visible in Fig. 1d and 1e are oxides which were formed during corrosion. Those corrosion products are dense and closely packed together. In Fig. 2a–c, the EDS results before immersion tests are presented. There is no presence of oxides visible. The high amount of oxygen is backed up by results visible in Fig. 2d–f, as compared to Fig. 2a–c, where only basic components can be seen. All samples contain 53.2 at.% of oxygen for the sample after 13 h, 56.3 for 20 h and 52.6 after 70 h, respectively. The EDS results indicate presence of Cl in case of all the samples and minuscule amount of K in the sample after 70 h. Those elements may be resulting from the Ringer solution, as it contains a high number of chlorides. When compared, the EDS results in Fig. 2d–f high amount of oxygen appears in the alloy, backing up the formation of various oxides. From the previous research, it is known that a $MgZn_2$ phase is present in the material [27]. The mechanism of corrosion of the $MgZn_2$ phase is known thanks to the literature, and it is said to be more stable as compared to pure Zn or Mg [33, 34]. The known corrosion behavior of the Mg alloys mentions the dissolution of Mg and creation of magnesium oxides (MgO and $Mg(OH)_2$) on the surface layer of the alloy [35]. Although the layer of magnesium oxides and hydroxides creates a passive layer, it is not a stable layer, as it is mentioned that the formation of stable passive layer is only possible in an alkaline environment devoid of aggressive chlorides [36]. However, a completely passive layer, as it happens with titanium for example, would make a biodegradable material impossible, thus the formation of the oxide/hydroxide layer, even though cyclic and temporary, deters immediate corrosion and slows down the process. Moreover, it was hypothesized the Clanions contribute to the dissociation of Mg layer. It may not affect the substitution on MgO or $Mg(OH)_2$ yet it stabilizes the intermediate forms of mentioned oxides, thus introducing some degree of passivity in the sample [35, 36].

What is important to mention, Zn forms similar oxides, although when paired with Mg, a preferential corrosion takes place, as Mg is a nobler metal. It is known, that during Mg

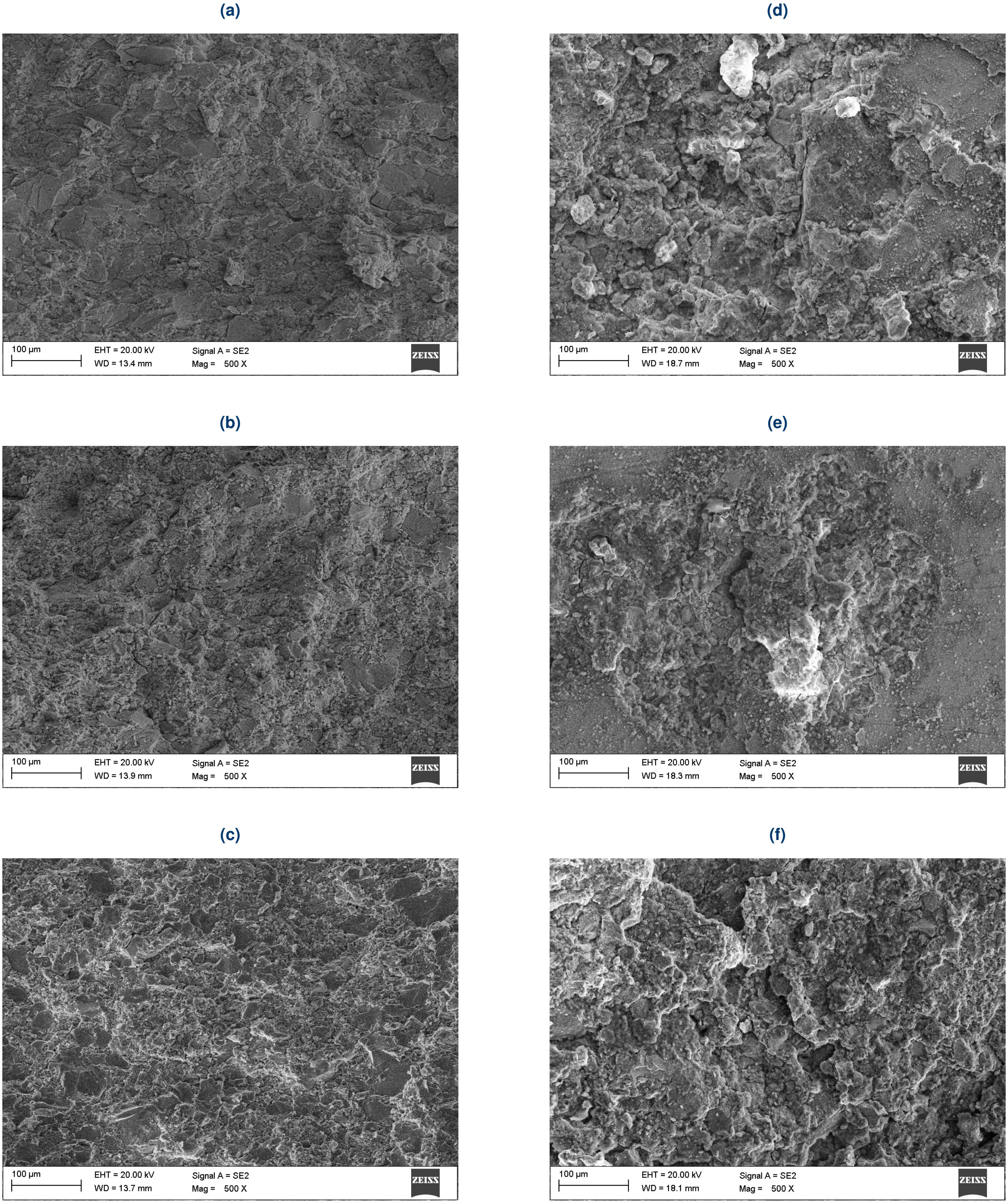

Fig. 1. SEM Micrographs of the sintered sample milled for 13, 20 and 70 h, before – (a), (b), (c) and after immersion tests – (d), (e), (f) respectively

hydrogen evolution occurs, promoting $Mg(OH)_2$. In neutral pH Zn forms a passive ZnO layer, although in the range of 4–10 pH it was reported that the ZnO layer has a pseudo-passive characteristic, hence not offering a reliable passivity to the alloy, although it still does slow down the corrosion process considerably [34].

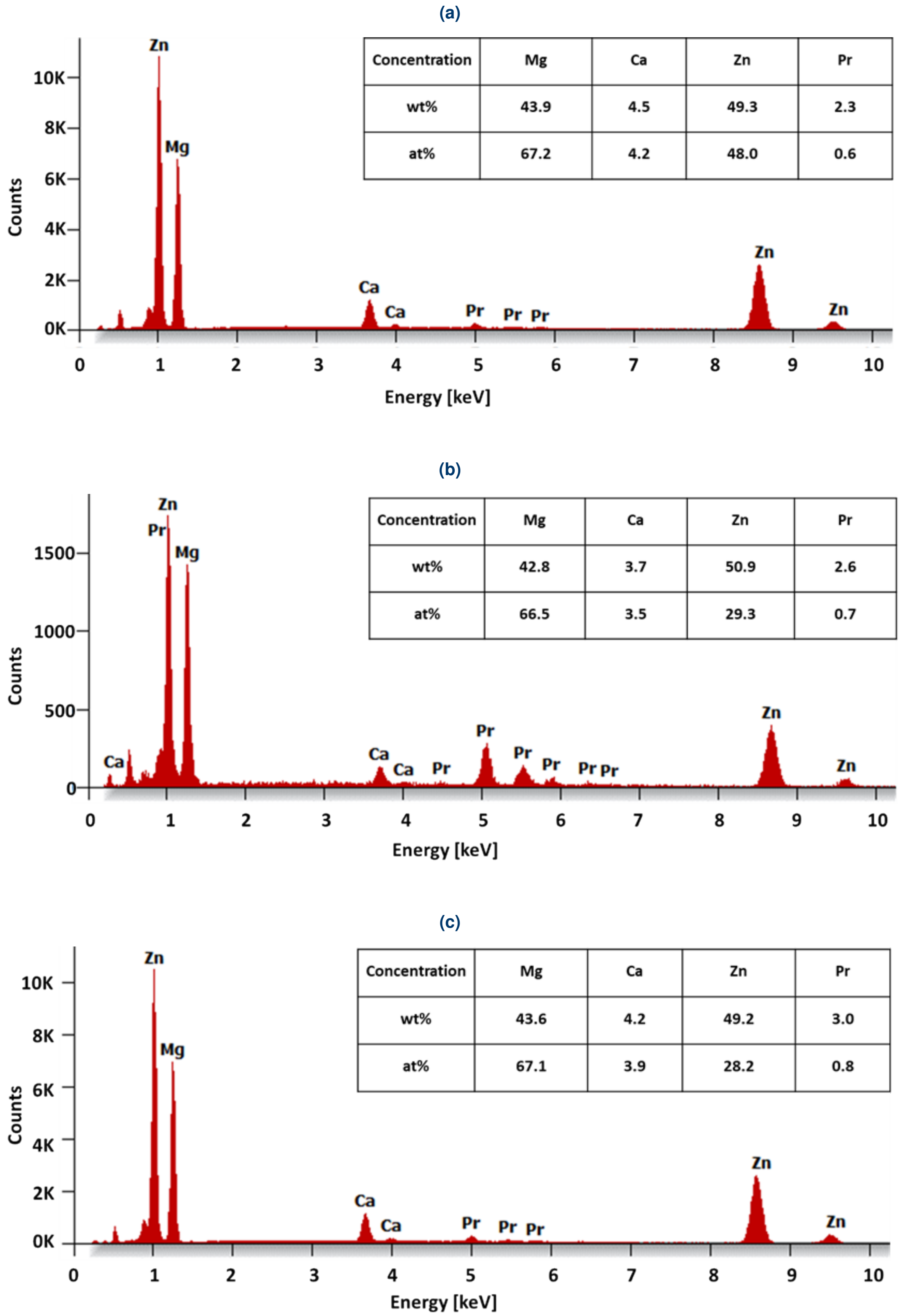

Fig. 2 (a)–(c)

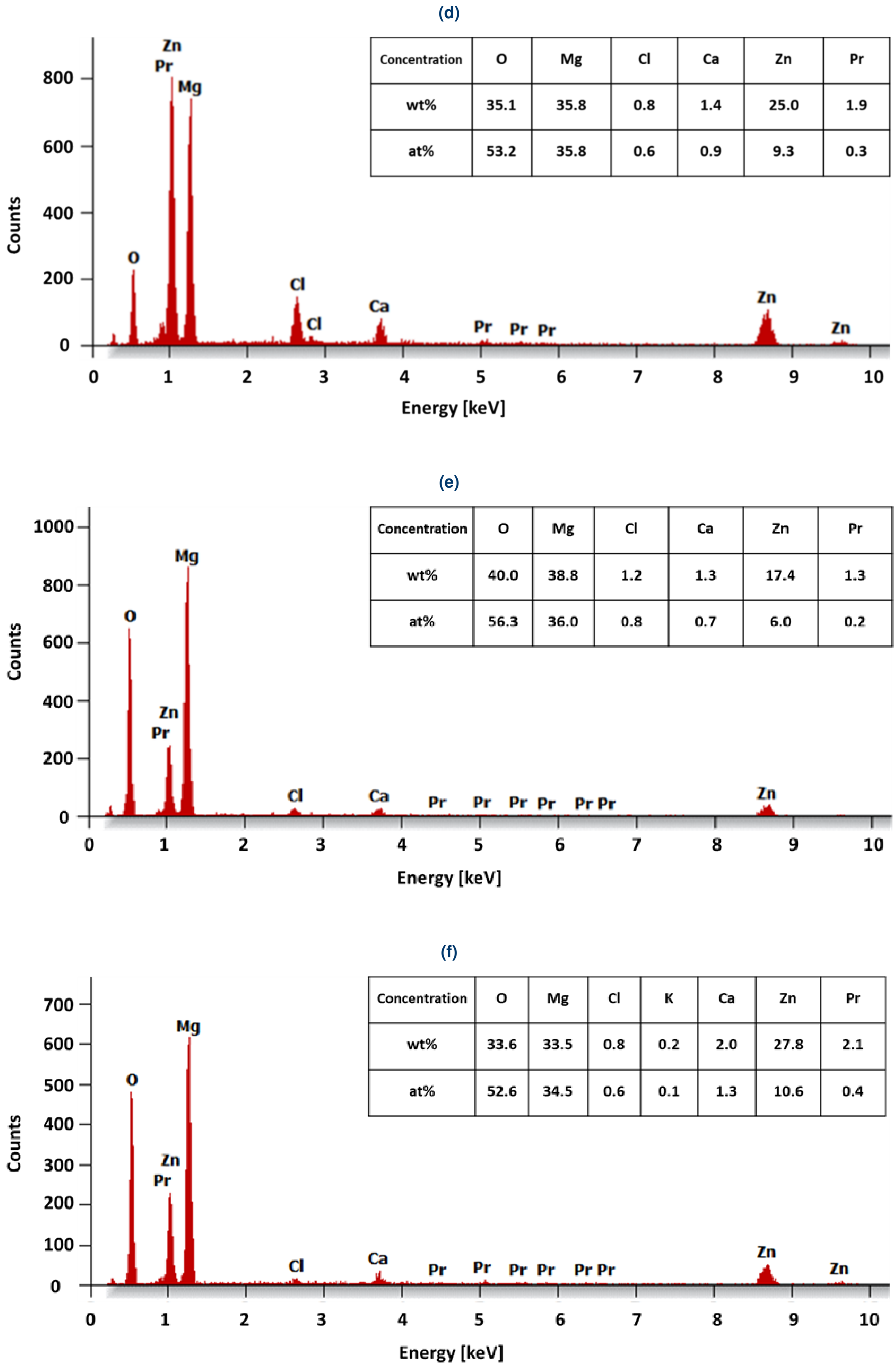

(d)

Concentration	O	Mg	Cl	Ca	Zn	Pr
wt%	35.1	35.8	0.8	1.4	25.0	1.9
at%	53.2	35.8	0.6	0.9	9.3	0.3

(e)

Concentration	O	Mg	Cl	Ca	Zn	Pr
wt%	40.0	38.8	1.2	1.3	17.4	1.3
at%	56.3	36.0	0.8	0.7	6.0	0.2

(f)

Concentration	O	Mg	Cl	K	Ca	Zn	Pr
wt%	33.6	33.5	0.8	0.2	2.0	27.8	2.1
at%	52.6	34.5	0.6	0.1	1.3	10.6	0.4

Fig. 2. EDS results and chemical compositions of the analyzed samples milled for 13, 20 and 70 h, before – (a), (b), (c) and after immersion tests – (d), (e), (f), respectively

3.2. Electrochemical corrosion

Figure 3a shows cases the open circuit potential E_{OCP} curves. This graph shows the tendency of the alloy to be subject to the electrochemical reactions happening in the cell environment. All samples take up to 600 s to stabilize, and then after 1200 s the changes are minimal, meaning some localized corrosion is happening, but most of the surface has reached a stable behavior, featuring some protective film resisting more aggressive corrosion. In Fig. 3b Tafel plots are presented, featuring the relation between the generated current and the electrode potential of tested alloy.

(a)

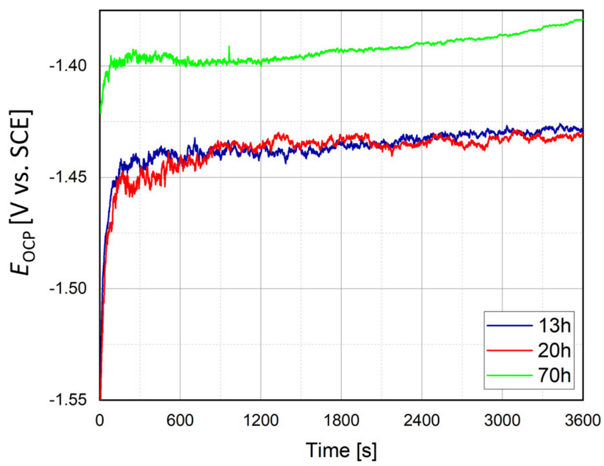

(b)

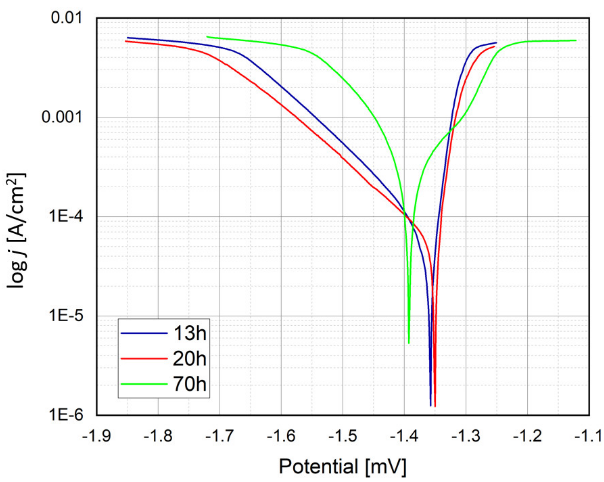

Fig. 3. E_{OCP} curves (a); Tafel plots for $Mg_{65}Zn_{30}Ca_4Pr_1$ alloy specimens subjected to immersion tests (b)

The sample after 13 h had –1.36 V of the corrosion potential, the highest value of –1.35 V was obtained for the $Mg_{65}Zn_{30}Ca_4Pr_1$ sample milled for 20 h, and the lowest of –1.39 V for the sample milled for 70 h (Fig. 3b). The results of the potentiodynamic testing are presented in Table 1 for clarity. The polarization resistance R_p was 144 Ω, 189 Ω, and 101 Ω for sintered $Mg_{65}Zn_{30}Ca_4Pr_1$ samples after milling 13, 20, and 70 h, respectively.

Table 1

Results of the potentiodynamic electrochemical tests for $Mg_{65}Zn_{30}Ca_4Pr_1$ alloy milled for 13, 20, and 70 h, respectively (E_{corr} – corrosion potential, J_{corr} – corrosion current density, i_{corr} – corrosion current, R_p – polarization resistance, E_{OCP} – open circuit potential)

Sample	E_{corr} (V)	J_{corr} (μA/cm^2)	i_{corr} (μA)	R_p (Ω)	E_{OCP} (V)
13 h	–1.36	87.00	87.00	144	–1.55
20 h	–1.35	57.25	57.25	189	–1.55
70 h	–1.39	201.17	201.17	101	–1.42

The presence of the amorphous phase in the material microstructure manufactured via MA may cause an increase in the porosity of the material during SPS process. It is caused by the presence of free volume in the amorphous structure. Intermetallic phases such as $MgZn_2$ and $Ca_2Mg_5Zn_{13}$ create micro-galvanic cells, which in result cause a decrease in corrosion resistance [32, 37]. These phases are usually a result of the sintering/heating process. Our previous work [27] characterizes the phase and chemical compositions and the morphology after three-point bending test. The microstructure of the Mg-Zn-Ca-Pr alloy presented in [27] features the differences between 13-, 20- and 70-hour samples in crystallite size and lattice strain. Although the phase composition of the analyzed samples is the same, those differences may cause the difference in the corrosion behavior. The porosity of the 70-hour samples is visible along with $MgZn_2$ crystallites and dispersed lighter lumps/dendrites of $Ca_2Mg_5Zn_{13}$ phase [27, 32]. Intermetallic phases, including hard, and brittle Laves phase with the characteristics typical for metallic state, decrease the corrosion resistance of the sample and its bending strength, although they increase its hardness considerably [27, 32]. Furthermore, the $MgZn_2$ Laves phase is more reactive and promotes thicker layers of corrosion products on its surface, due to the preferential corrosion of Mg over Zn, leading to passive layer, although only locally [38]. This can explain the difference in the Tafel diagrams presented in Fig. 3b.

4. CONCLUSIONS

In our study, $Mg_{65}Zn_{30}Ca_4Pr_1$ samples were milled for 13, 20, and 70 h respectively, compressed with 50 MPa of force and sintered at 350°C by SPS method. Their corrosion behavior in Ringer's solution has been studied.

Based on the electrochemical test results, it can be stated the corrosion resistance is related to the milling time.

Samples milled for 13 h (–1.36 V) and 20 h (–1.35 V) have similar values of corrosion potential, although they considerably differ in polarization resistance R_p with values of 144 Ω for 13 h and 189 Ω for 20 h. Those differences result in better corrosion resistance for the sintered sample milled for 20 h as compared to the sample milled for 13 h. The sintered sample milled for 70 h had the lowest values of –1.39 V and 101 Ω.

After immersion tests, the pitting corrosion was assessed via microscopic analysis of the samples surface morphology. Small cracks and pits were observed.

The differences in the corrosion behavior are caused by the $MgZn_2$ and $Ca_2Mg_5Zn_{13}$ intermetallic phases crystallite sizes and lattice strains present in the samples' microstructure as well as their porosity.

The corrosion mechanism is caused by the dissolution of the $MgZn_2$ and Mg phases into MgO and $Mg(OH)_2$ assisted by the Cl^- anions, creating a pseudo-passive layer on the sample surface, partially inhibiting deeper corrosion. At the Ringer's solution pH value, the Zn addition is contributing to further slowing down the corrosion rate. The possible corrosion products hinted by the EDS results are the alloy constituent oxides and hydroxides either precipitating from the solution or deploying on the sample surface.

ACKNOWLEDGEMENTS

This research was funded by the National Science Center, Poland, grant number 2017/27/B/ST8/02927.

REFERENCES

[1] X. Liu, W. Yuan, D. Shen, Y. Cheng, D. Chen, and Y. Zheng, "Exploring the biodegradation of pure Zn under simulated inflammatory condition," *Corros. Sci.*, vol. 189, p. 109606, Aug. 2021, doi: 10.1016/J.CORSCI.2021.109606.

[2] Z. Zhang *et al.*, "Zn0.8Li0.1Sr – a biodegradable metal with high mechanical strength comparable to pure Ti for the treatment of osteoporotic bone fractures: In vitro and in vivo studies," *Biomaterials*, vol. 275, p. 120905, Aug. 2021, doi: 10.1016/ J.BIOMATERIALS.2021.120905.

[3] F. Witte, "The history of biodegradable magnesium implants: A review," *Acta Biomater.*, vol. 6, no. 5, pp. 1680–1692, May 2010, doi: 10.1016/J.ACTBIO.2010.02.028.

[4] Y.B. Wang *et al.*, "Biodegradable CaMgZn bulk metallic glass for potential skeletal application," *Acta Biomater.*, vol. 7, no. 8, pp. 3196–3208, Aug. 2011, doi: 10.1016/j.actbio.2011.04.027.

[5] D. Persaud-Sharma and A. Mcgoron, "Biodegradable magnesium alloys: A review of material development and applications," *J. Biomim. Biomater. Tissue. Eng.*, vol. 12, no. 1, pp. 25–39, 2012, doi: 10.4028/www.scientific.net/JBBTE.12.25.

[6] D. Jain *et al.*, "Effect of exposure time on corrosion behavior of zinc-alloy in simulated body fluid solution: Electrochemical and surface investigation," *J. Mater.s Res. Technol.*, vol. 10, pp. 738–751, Jan. 2021, doi: 10.1016/J.JMRT.2020.12.050.

[7] M.K. Datta *et al.*, "Structure and thermal stability of biodegradable Mg–Zn–Ca based amorphous alloys synthesized by mechanical alloying," *Mater. Sci. Eng. B*, vol. 176, no. 20, pp. 1637–1643, Dec. 2011, doi: 10.1016/J.MSEB.2011.08.008.

[8] B. Hrapkowicz and S.T. Lesz, "Characterization of $Ca_{50}Mg_{20}Zn_{12}Cu_{18}$ Alloy," *Arch. Foundry Eng.*, vol. 19, no. 1, pp. 75–82, 2019, doi: 10.24425/AFE.2018.125195.

[9] Z. Li, X. Gu, S. Lou, and Y. Zheng, "The development of binary Mg–Ca alloys for use as biodegradable materials within bone," *Biomaterials*, vol. 29, no. 4, pp. 1329–1344, 2008, doi: 10.1016/ j.biomaterials.2007.12.021.

[10] B. Hrapkowicz, S. Lesz, M. Karolus, J. Popis, and A. Gabryś, "Electrochemical Behaviour and Morphology of Selected Sintered Samples of $Mg_{65}Zn_{30}Ca_4Pr_1$ Alloy," in *International Conference – Material Technologies in Silesia'2022*, Jun. 2022, pp. 63–64.

[11] B.S. Murty, M.K. Datta, and S.K. Pabi, "Structure and thermal stability of nanocrystalline materials," *Sadhana*, vol. 28, no. 1, pp. 23–45, 2003, doi: 10.1007/BF02717124.

[12] M.B. Kannan and R.K.S. Raman, "In vitro degradation and mechanical integrity of calcium-containing magnesium alloys in modified-simulated body fluid," *Biomaterials*, vol. 29, no. 15, pp. 2306–2314, 2008, doi: 10.1016/j.biomaterials.2008.02.003.

[13] B. Zberg, P.J. Uggowitzer, and J.F. Löffler, "MgZnCa glasses without clinically observable hydrogen evolution for biodegradable implants," *Nat. Mater.*, vol. 8, no. 11, pp. 887–891, Nov. 2009, doi: 10.1038/nmat2542.

[14] J.H. Byrne, E.D. O'Cearbhaill, and D.J. Browne, "Comparison of crystalline and amorphous versions of a magnesium-based alloy: corrosion and cell response," *Eur. Cell Mater.*, vol. 30, no. S.3, p. 75, 2015.

[15] H.E. Friedrich and B.L. Mordike, "Magnesium technology: Metallurgy, design data, applications," in *Magnesium Technology: Metallurgy, Design Data, Applications*, Springer Berlin, Heidelberg, 2006, pp. 1–677, doi: 10.1007/3-540-30812-1.

[16] N. Žaludová, "Mg-RE Alloys and Their Applications," *WDS'05 Proceedings of Contributed Papers*, 2005, pp. 643–648.

[17] K. Kowalski, M. Nowak, J. Jakubowicz, and M. Jurczyk, "The Effects of Hydroxyapatite Addition on the Properties of the Mechanically Alloyed and Sintered Mg-RE-Zr Alloy," *J. Mater. Eng. Perform.*, vol. 25, no. 10, pp. 4469–4477, Oct. 2016, doi: 10.1007/s11665-016-2306-y.

[18] D. Liu, D. Yang, X. Li, and S. Hu, "Mechanical properties, corrosion resistance and biocompatibilities of degradable Mg-RE alloys: A review," *J. Mater. Res. Technol.*, vol. 8, no. 1, pp. 1538–1549, 2019, doi: 10.1016/j.jmrt.2018.08.003.

[19] S. Lesz, B. Hrapkowicz, M. Karolus, and K. Gołombek, "Characteristics of the Mg-Zn-Ca-Gd Alloy after Mechanical Alloying," *Materials*, vol. 14, no. 226, p. 226, 2021, doi: 10.3390/ ma14010226.

[20] S. Lesz, B. Hrapkowicz, K. Gołombek, M. Karolus, and P. Janiak, "Synthesis of Mg-based alloys with rare-earth element addition by means of mechanical alloying," *Bull. Pol. Acad. Sci. Tech. Sci.*, vol. 69, no. 5, p. e137586, 2021, doi: 10.24425/ BPASTS.2021.137586.

[21] B. Cao *et al.*, "The Accumulation and Metabolism Characteristics of Rare Earth Elements in Sprague-Dawley Rats," *Int. J. Environ. Res. Public Health*, vol. 17, p. 1399, 2020, doi: 10.3390/ijerph17041399.

[22] R. Leggett, E. Ansoborlo, M. Bailey, D. Gregoratto, F. Paquet, and D. Taylor, "Biokinetic data and models for occupational intake of lanthanoids," *Int. J. Radiat. Biol.*, vol. 90, no. 11, pp. 996–1010, 2014, doi: 10.3109/09553002.2014.887868.

[23] P.W. Durbin, M.H. Williams, M. Gee, R.H. Newman, and J.G. Hamilton, "Metabolism of the Lanthanons in the Rat," *Exp. Biol. Med.*, vol. 91, no. 1, pp. 78–85, Nov. 2016, doi: 10.3181/ 00379727-91-22175.

[24] B. Lindell and F.D. Sowby, *Limits for Intakes of Radionuclides by Workers*, vol. 2, no. 3/4. Oxford, New York, Frankfurt: Pergamon Press, 1979.

[25] K. Amiya and A. Inoue, "Formation, Thermal Stability and Mechanical Properties of Ca-Based Bulk Glassy Alloys," *Mater. Trans.*, vol. 43, no. 1, pp. 81–84, 2002, doi: 10.2320/matertrans.43.81.

[26] I. Polmear, D. StJohn, J.-F. Nie, and M. Qian, "Novel Materials and Processing Methods" in *Light Alloys (Fifth Edition)*, Butterworth-Heinemann: Boston, 2017, doi: 10.1016/b978-0-08-099431-4.00008-7.

[27] B. Hrapkowicz *et al.*, "Microstructure and Mechanical Properties of Spark Plasma Sintered Mg-Zn-Ca-Pr Alloy," *Metals*, vol. 12, no. 3, p. 375, Feb. 2022, doi: 10.3390/MET12030375.

[28] J. Trapp and B. Kieback, "Fundamental principles of spark plasma sintering of metals: part I – Joule heating controlled by the evolution of powder resistivity and local current densities," *Powder Metall.*, vol. 62, no. 5, pp. 297–306, Oct. 2019, doi: 10.1080/00325899.2019.1653532.

[29] R. Orrù, R. Licheri, A.M. Locci, A. Cincotti, and G. Cao, "Consolidation/synthesis of materials by electric current activated/assisted sintering," *Mater. Sci. Eng. R-Rep.*, vol. 63, no. 4–6, pp. 127–287, Feb. 2009, doi: 10.1016/J.MSER.2008.09.003.

[30] L. Schultz, "Formation of amorphous metals by mechanical alloying," *Mater. Sci. Eng.*, vol. 97, no. C, pp. 15–23, Jan. 1988, doi: 10.1016/0025-5416(88)90004-3.

[31] C. Suryanarayana, "Mechanical alloying and milling," *Prog. Mater. Sci.*, vol. 46, no. 1–2, pp. 1–184, Jan. 2001, doi: 10.1016/S0079-6425(99)00010-9.

[32] Y.F. Zhao, J.J. Si, J.G. Song, and X.D. Hui, "High strength Mg-Zn-Ca alloys prepared by atomization and hot pressing process," *Mater. Lett.*, vol. 118, pp. 55–58, 2013, doi: 10.1016/j.matlet.2013.12.053.

[33] J. Han and K. Ogle, "Dealloying of $MgZn_2$ Intermetallic in Slightly Alkaline Chloride Electrolyte and Its Significance in Corrosion Resistance," *J. Electrochem. Soc.*, vol. 164, no. 14, p. C952, Nov. 2017, doi: 10.1149/2.0341714JES.

[34] A.I. Ikeuba *et al.*, "Understanding the electrochemical behavior of bulk-synthesized $MgZn_2$ intermetallic compound in aqueous NaCl solutions as a function of pH," *J. Solid State Electrochem.*, vol. 23, no. 4, pp. 1165–1177, Apr. 2019, doi: 10.1007/S10008-019-04210-Y.

[35] C.L. Wetteland, J. de Jesus Sanchez, C.A. Silken, N.Y.T. Nguyen, O. Mahmood, and H. Liu, "Dissociation of magnesium oxide and magnesium hydroxide nanoparticles in physiologically relevant fluids," *J. Nanopart. Res.*, vol. 20, no. 8, pp. 1–17, Aug. 2018, doi: 10.1007/S11051-018-4314-3/FIGURES/6.

[36] S. Virtanen, "Biodegradable Mg and Mg alloys: Corrosion and biocompatibility," *Mater. Sci. Eng. B*, vol. 176, no. 20, pp. 1600–1608, Dec. 2011, doi: 10.1016/J.MSEB.2011.05.028.

[37] Y.N. Zhang, X.D. Liu, Z. Altounian, and M. Medraj, "Coherent nanoscale ternary precipitates in crystallized Ca4Mg72Zn24 metallic glass," *Scr. Mater.*, vol. 68, no. 8, pp. 647–650, Apr. 2013, doi: 10.1016/J.SCRIPTAMAT.2012.12.028.

[38] E. Diler *et al.*, "Initial formation of corrosion products on pure zinc and $MgZn_2$ examinated by XPS," *Corros. Sci.*, vol. 79, pp. 83–88, Feb. 2014, doi: 10.1016/J.CORSCI.2013.10.029.